

: 가<sup>1</sup>

Figure 1 is a line graph showing the number of cases of COVID-19 in the United States from March 2020 to March 2021. The x-axis represents time in months, and the y-axis represents the number of cases. The graph shows a sharp increase in cases starting in March 2020, peaking in April 2020, and then a gradual decline. A horizontal line at 100,000 cases is labeled '3'. A vertical line at approximately 100,000 cases is labeled '2'.

Q 가 30, 70, 120 3 가 32 JPEG (Joint Photographic Expert Group) 96 3 가 가 , 2 가 가 , 5 가 가 2 가 Q 30 가 Q 70 120 Q 70 15 , Q 120 35 Q 30 Q 70 120 가 가 가

가 . PACS (Picture Archiving and Communication System)가  
가

가    가    ,  
      가

가 .

가

1998 2 1 8 31 X-  
(FCR 9000, Fuji Photo Film Co Ltd., Japan)  
32

(1-8).

가  
(1, 2).

. PACS

[illegible]

3 가 , (A, B) 가  
 22:1, 51:1, 95:1 6557 - 9806  
 KB 7358 KB Microsoft 100  
 NT (Microsoft, Redmond, WA, U.S.A.) ft-lambert  
 IBM , Pentium Pro- 가  
 200MHz, 128 MB 가  
 32 - Q30 (Q30 ), 32 가  
 - Q70 (Q70 ), 32 - Q120 가  
 (Q120 ), 96 2 가 가 2  
 . 2 (2048 × 2560 , 3 가  
 Dataray Corp., Denvor, U.S.A.) , ,

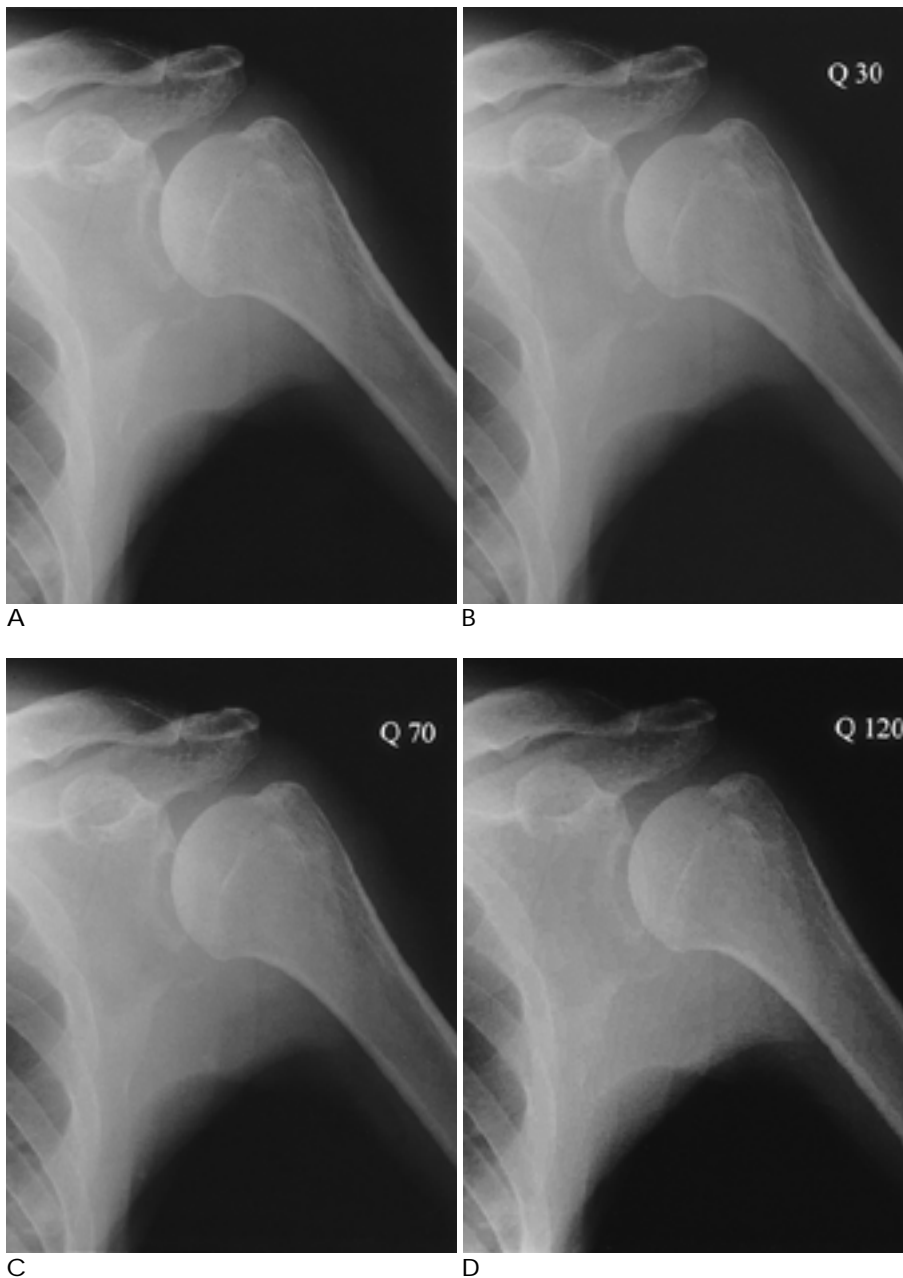


Fig. 1. Metastasis in the scapula  
 Destructive bony lesion is seen at the lateral border of the scapula. Compressed image with Q factor 30 (B) reveals no perceptible difference comparing with uncompressed image (A). Compressed images with Q factor 70 and 120 (C and D) show relatively poor definition of the lesion. Linear opacities such as rib margins are blurred, and soft tissue densities are inhomogeneous in C and D.

(trabeculae) 가 . 가 .

가 . 3 가 가 .

가 . 가 .

A2: A B . 2 가  
A1: A B . 0.5 ,  
0 : A, B 가 . 가 0.5  
B1: A B .  
B2: A B . binomial dis-  
tribution test .

가 가 가 .  
32 3

- Q120 가 . 가

가 가 . 3 3 가 Table 1 - 3  
가 가 , 가 . Q30 가 가  
. A, B .  
Q70 Q120 3 가 .  
가

-2: (Table 1). Q30 3  
-1: 가 -  
0: 가 가 가 . Q70 Q120 3  
1: 가  
2: 가 . Q70 Q120  
Wilcoxon signed-rank test 3 가 가

Table 1. Tumor-related Features

	Reader 1					Reader 2					Reader 3				
	-2	-1	0	1	2 *	-2	-1	0	1	2	-2	-1	0	1	2
UC: Q30 CM	1	4	20	7	0	1	5	22	3	1	0	0	30	2	0
UC: Q70 CM	0	1	7	16	8	0	2	16	7	7	0	0	18	12	2
UC: Q120 CM	0	0	5	6	21	1	0	2	13	16	0	0	11	13	8

UC: uncompressed image

CM: compressed image

\* -2: Uncompressed image is inferior to compressed image.

-1: Uncompressed image may be inferior to compressed image.

0: Uncompressed image is equal to compressed image.

1: Uncompressed image may be superior to compressed image.

2: Uncompressed image is superior to compressed image.

Table 2. Linear Structures

	Reader 1					Reader 2					Reader 3				
	-2	-1	0	1	2 *	-2	-1	0	1	2	-2	-1	0	1	2
UC: Q30 CM	1	1	26	4	0	2	8	15	6	1	0	1	27	4	0
UC: Q70 CM	0	1	11	12	8	0	4	9	9	10	0	1	13	13	5
UC: Q120 CM	0	0	0	8	24	1	0	0	4	27	0	1	4	12	15

UC: uncompressed image

CM: compressed image

\* same as in table 1.

(Table 2, 3). Q30 2 3 가 Q120 2  
 1  
 가  
 가 가  
 . 3 가  
 가 Q30 3 가  
 가 Q70  
 가  
 Q70 Q120 3 가  
 가 Q70  
 가 96

Table 3. Soft Tissue Homogeneity

	Reader 1					Reader 2					Reader 3				
	-2	-1	0	1	2 *	-2	-1	0	1	2	-2	-1	0	1	2
UC: Q30 CM	1	4	20	7	0	5	11	8	3	5	1	1	22	8	0
UC: Q70 CM	0	0	8	11	13	0	3	3	6	20	0	0	6	14	12
UC: Q120 CM	0	0	3	4	25	1	0	0	2	29	0	0	1	3	28

UC: uncompressed image

CM: compressed image

\* same as in table 1.

Table 4. Frequency of Selections as a Better One in Each Pair of Uncompressed and Compressed Images. (binomial distribution test)

	Reader 1			Reader 2			Reader 3			All readers		
UC: Q30 CM	21:	11	(.112)	12:	20	(.216)	21:	11	(.112)	54:	42	(.262)
UC: Q70 CM	30:	2	(.000)	27:	5	(.000)	30:	2	(.000)	87:	9	(.000)
UC: Q120 CM	30:	2	(.000)	31:	1	(.000)	32:	0	(.000)	93:	3	(.000)

UC: uncompressed image

CM: compressed image

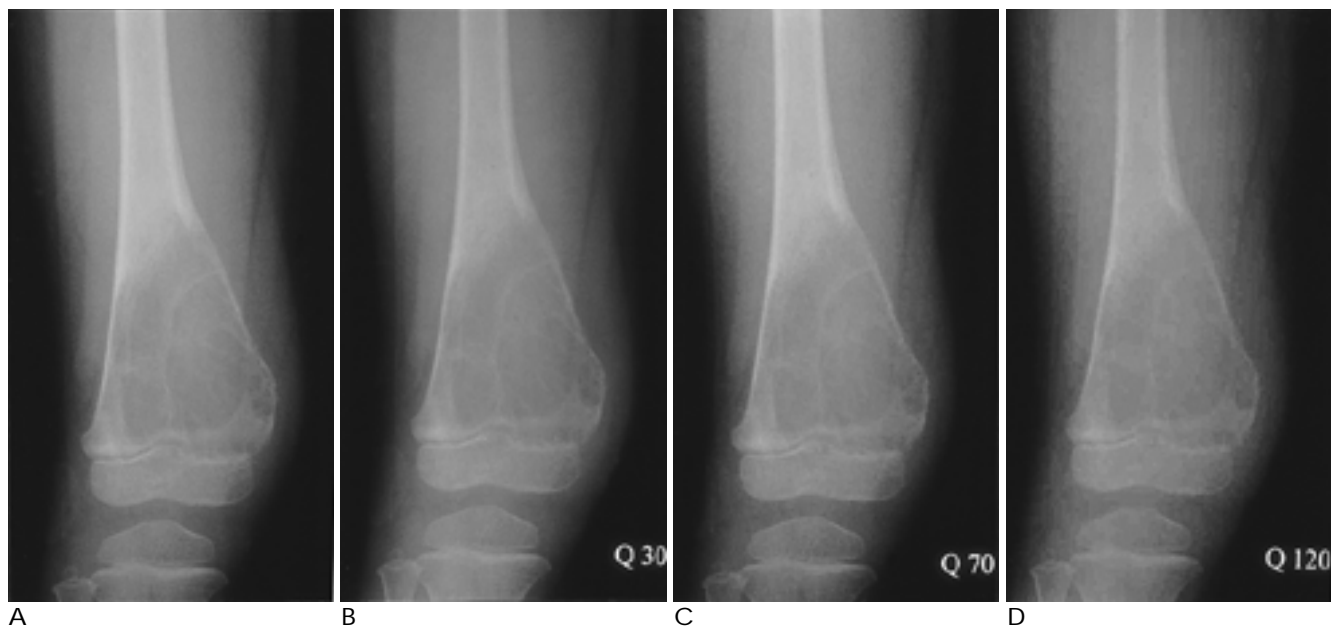


Fig. 2. Aneurysmal bone cyst in the distal femur.

There is no identifiable difference between uncompressed (A) and compressed image with Q factor 30 (B). On compressed image with Q factor 120 (D), border of the lesion is more indistinct than on A and B, internal trabeculations are fuzzy, and soft tissues are inhomogeneous. To lesser degree, compressed image with Q factor 70 (C) also shows these patterns of image degradation.



(  
),  
가  
(geographic),  
(moth-eat-  
(permeative)가  
,  
(12).  
Q70 Q120  
96 15 , Q120 35  
Q120 가 가 . 가  
가 가 Q120  
(Fig. 3). 가  
JPEG Q  
30 ( 22:1) Q 70 ( 51:1)  
Q 120 ( 95:1) 가

Goldberg (1)

Q120

1. Goldberg MA, Pivovarov M, Mayo-Smith WW, Bhalla MP, Blickman JG, Bramson RT, Boland GWL, Llewellyn HJ, Halpern E. Application of wavelet compression to digitalized radiographs. *AJR* 1994;163:463-468
2. Bramble JM, Huang HK, Murphy MD. Image data compression. *Invest Radiol* 1988;23:707-712
3. Cosman PC, Davidson HC, Bergin CJ, Tseng CW, Meses LE, Riskin EA, Olshen RA, Gray RM. Thoracic CT images: effect of lossy image compression on diagnostic accuracy. *Radiology* 1994;190:517-524
4. Aberle DR, Gleeson F, Sayre JW, Brown K, Batra P, Young DA, Stewart BK, Ho BKT, Huang HK. The effect of irreversible image compression on diagnostic accuracy in thoracic imaging. *Invest Radiol* 1993;28:398-403
5. MacMahon H, Doi K, Sanada S, Montner SM, Giger ML, Metz CE, Nakamori N, Yin FF, Xu XW, Yonekawa H, Takeuchi H. Data compression: effect on diagnostic accuracy in digital chest radiog-

- raphy. *Radiology* 1991;178:175-179
6. Ishigaki T, Sakuma S, Ikeda M, Itoh Y, Suzuki M, Iwai S. Clinical evaluation of irreversible image compression: analysis of chest imaging with computed radiography. *Radiology* 1990;175:739-743
  7. Erickson BJ, Manduca A, Persons KR, Earnest F, Hartman TE, Harms GF, Brown LR. Evaluation of irreversible compression of digitized posterior-anterior chest radiographs. *J Digit Imag* 1997;10: 97-102
  8. Lo S-C, Huang HK. Compression of radiological images with 512, 1024, 2048 matrices. *Radiology* 1986;161:519-525
  9. Ho BKT, Tseng V, Ma M, Chen D. A mathematical model to quantify JPEG block artifacts. *Proc SPIE* 1993;1897:269-274
  10. MacMahon H, Vvborny C, Metz CE, Doi K, Sabeti V, Solomon SL. Digital radiography of subtle pulmonary abnormalities: an ROC study of the effect of pixel size on observer performance. *Radiology* 1986;158:21-26
  11. Gur D, Rubin DA, Kart BH, Peterson AM, Fuhrman DR, Rockette HE, King JL. Forced choice and ordinal discrete rating assessment of image quality: a comparison. *J Digit Imag* 1997;10:103-107
  12. Resnick D. *Tumors and tumor-like diseases. In bone and joint imaging*. 2nd ed. W.B. Saunders Company 1996:979-987

J Korean Radiol Soc 1999;41:611-617

## Computed Radiography in Skeletal Imaging: Visual Assessment of Compressed Image Quality<sup>1</sup>

Sung Hwan Hong, M.D., Jong Hyo Kim, Ph.D., Jin Mo Goo, M.D., Jung-Eun Cheon, M.D.,  
Young Hoon Kim, M.D., Dong Kyung Lee, M.D., Joo Hee Cha, M.D., Chi Sung Song, M.D.<sup>3</sup>,  
Yong Seok Kim<sup>2</sup>, Heung Sik Kang, M.D., Man Chung Han, M.D.

<sup>1</sup>Department of Radiology, Seoul National University College of Medicine

<sup>2</sup>Seoul National University Hospital Medical Informatics Center

<sup>3</sup>Department of Radiology, Boramae City Hospital

**Purpose :** To evaluate the effect of lossy image compression on skeletal images and to determine the compression ratio which does not lead to difficulties when images are interpreted for diagnostic purposes.

**Materials and Methods :** Thirty-two computed radiographs (CR) of osteolytic bone tumors were obtained from Picture Archiving and Communication System. They were compressed to three different levels (Q factor 30, 70, 120) using the JPEG (Joint Photographic Expert Group) technique. Ninety-six pairs of uncompressed and compressed images were randomly ordered and then serially displayed on two high-resolution monitors. During a side-by-side review, three radiologists independently compared each pair of uncompressed and compressed images, and these were rated once using a five-category ordinal scale for tumor-related findings, linear structures, and soft tissues. The reviewers were then obliged to decide which image in each pair was of better quality, and finally, they were asked to evaluate the influence of image compression on diagnostic accuracy.

**Results :** The reviewers found no significant difference in image quality between uncompressed and compressed images with a Q factor 30. Compressed images with a Q factor of 70 or 120, however, revealed clinically relevant degradation. Among 96 observations of compressed images, 15 with a Q factor of 70 and 35 with a Q factor of 120 were considered inadequate for clinical purposes.

**Conclusion :** If the JPEG technique is used, compressed CR skeletal images with a Q factor of 30 are acceptable for clinical application. Compressed images with a Q factor of 70 or 120 may, however, cause diagnostic difficulty and thus cannot be used for clinical purposes.

**Index words :** Images, quality  
Images, processing  
Radiography, digital

Address reprint requests to : Jong Hyo Kim, Ph.D., Department of Diagnostic Radiology, Seoul National University Hospital  
#28 Yongon-dong, Chongno-gu, Seoul, 110-744, Korea.  
Tel. 82-2-760-3677 Fax. 82-2-743-6385